Natural Landmark Based Localisation of Mobile Robots Using Laser Range Data

Maria Isabel Ribeiro
Instituto Superior Técnico and
Instituto de Sistemas e Robótica
Av.Rovisco Pais, 1
P-1096 Lisboa CODEX, PORTUGAL
e-mail: mir @ isr.ist.utl.pt

João G.M. Gonçalves
European Commission, Joint Research Centre
Institute for Systems, Informatics and Safety
21020 Ispra (VA), ITALY
e-mail: joao.goncalves @jrc.it

Abstract

This paper presents a localisation procedure for a mobile robot operating in a structured environment whose map is totally or partially known a priori. The proposed approach is based on the recognition of natural landmarks identified through Laser Range data.

With a rough estimate of the robot's position and orientation and the knowledge of an a priori map, the proposed technique chooses two vertical edges toward which, and using correctly chosen scanning parameters, a laser scan is directed. The post-processing of the so acquired range profile results in an updated estimate of the robot's location. The paper describes the different steps of the localisation technique, derives a criterion for the optimal choice of the pair of vertical edges, discusses relevant experimental results and presents directions for further research.

1. Problem formulation

One of the major problems in autonomous navigation of a mobile robot is the determination of its position and orientation relative to a pre-defined frame. This is an important issue in certain types of applications and various approaches have been proposed to solve it, namely dead reckoning and reference guidance supported on beacon and landmark estimators or on model based estimators. In [3] the most common sensors and methods for mobile robot positioning are surveyed.

In what concerns the reference guidance with beacons or landmarks, some localisation techniques require additional external installations such as transmitters, marks, reflectors, etc., [6]. A number of works, however, have been proposed that do not require environment modifications. For example, in [2] and [9] the location estimate is obtained through the matching between an a priori map and a 2D profile of range data obtained from a complete (360 degrees) scan of the environment taken from the mobile robot. A different approach in this same category, but avoiding the requirement of an entire scan, extracts features from the environment and match them with an a priori map. The works [1], [5], [7] follow this approach using ultrasonic range sensors.

The localisation approach described in this paper is based on the recognition of natural landmarks and although requiring feature extraction is not a feature based approach. The procedure, aiming at running while the vehicle is moving, estimates its location relative to a set of natural landmarks identified through Laser Range data. The a priori knowledge of a 3D map of the environment is available and no artificial landmarks need to be installed.

During the vehicle operation it is assumed that a dead-reckoning system provides a rough estimate of the robot position and orientation. With this estimate and the knowledge of the a priori map, the algorithm chooses the best landmarks that will be used for localisation updating and a laser scan directed towards those landmarks is performed. The so acquired range profile and the parameters of the scanning device lead to the estimation of the vehicle location through a circle intersection and a coordinate transformation. The so obtained vehicle location can be used for calibration of the odometric system, resetting therefore the inevitable odometric cumulative errors.

The paper is organised as follows. Section describes the world model, the experimental set-up and the various frames adopted along the work. Section 3 presents the various steps of the localisation technique. Section 4 derives an optimisation criterion for the choice of a pair of vertical edges for localisation purposes and discusses the estimation degradation when this choice is not available. Relevant experimental results, obtained for a robot in various fixed positions and orientations are displayed and discussed in Section 5. Conclusions and directions for future work are drawn in Section 6.

2. Notation and experimental set-up

A 3D description of the environment, described in terms of its contents, is assumed to be known a priori. The room contours, the doors, the walls and the windows are represented as polylines while the objects are described in terms of their polygonal base. In both cases, the total height and the height of its base are specified. As the localisation algorithm chooses natural landmarks among those to be considered in the world model, a post-processing on the map can exclude those features that will never be chosen as landmarks for localisation purposes. For example, as vertical edges are used by the localisation algorithm all other features can be withdrawn. Also, vertical edges that might, will high probability, be occluded by unexpected obstacles not represented in the a priori map might be excluded from the set of landmarks used for localisation purposes.

The experimental set-up is represented in Fig. 2.1.

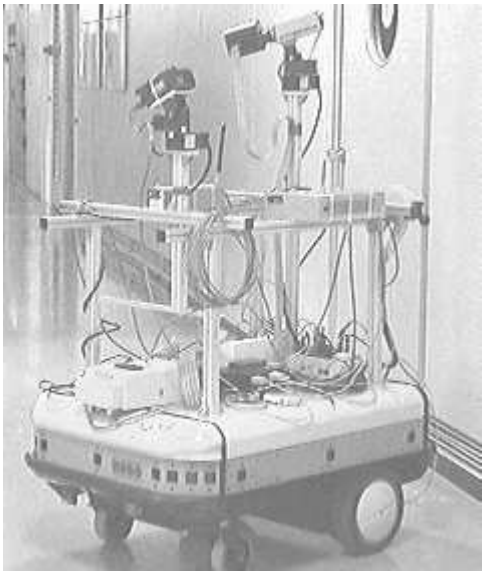

Figure 2.1 - Scanning device (LRF+PTU) mounted on the Robuter robot

The Robuter mobile robot is equipped with a main processor (68020@16MHz) where all the software for data acquisition and processing runs. The scanning device composed by a Laser Range Finder (LRF) mounted on a Pan and Tilt Unit (PTU) is fixed on a metallic structure attached to the base of the mobile robot. Range profiles are acquired within a user-established solid angle and distances measured on a grid with equally spaced pan angles and constant tilt angles. The scanning device has a pan range $\theta_1 \in [-140^o, 140^o]$ and a tilt range $\theta_2 \in [-30^o, 46^o]$. For a fixed position and orientation of its base, the pan range determines that a region of the environment, named as the shadow region of the PTU, cannot be scanned. This fact will be taken into account on the choice of the landmarks used for the localisation procedure. The LRF uses an eye safe laser beam with 4cm diameter and a divergence of 0.16^o. It has a distance range from 1 to 20m and a measurement resolution of about 2cm.

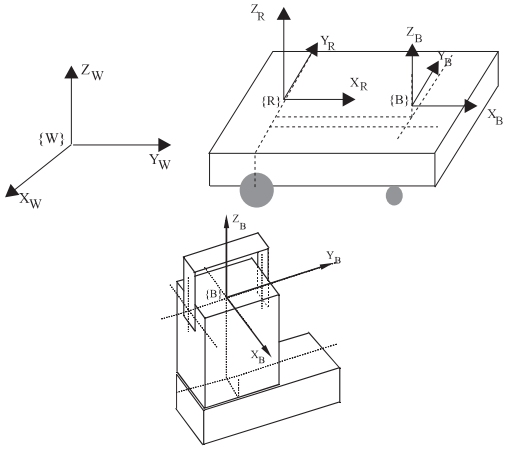

Fig.2.2 - World frame, {W}, robot frame, {R}, frame {B} associated to a reset PTU

Along the paper the environment map is described in the world frame {W}, a robot frame {R} is linked to the mobile robot, and a frame {B} is attached to the PTU in a reset situation (see Fig.2.2). For the sake of simplicity of the paper's presentation, and although the above referred are 3D frames, as the height of the vehicle is constant, the environment is considered flat and the base of the PTU is fixed on the vehicle's structure, the z coordinate will not be explicitly considered.

The robot location, at a given time instant, is represented by the triplet ${}^W u_R=(x_R,y_R,\theta_R)$, (see Fig.2.3) where (x_R, y_R) is the position and θ_R the orientation in the world frame.

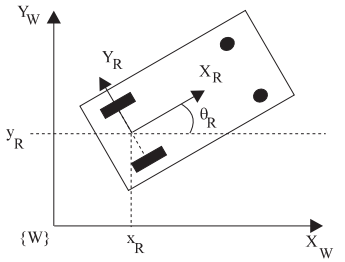

Fig.2.3 - Robot location in the world frame

Along this work, we will assume that the robot's location estimate is a random vector with a three dimensional Gaussian probability density function (pdf), with covariance matrix ${}^W\Lambda_R$ of the form,

$$ {}^W\Lambda_R = \begin{bmatrix} \sigma^2_{x_R} & \sigma_{x_R y_R} & \sigma_{x_R \theta_R} \\ \sigma_{x_R y_R} & \sigma^2_{y_R} & \sigma_{y_R \theta_R} \\ \sigma_{x_R \theta_R} & \sigma_{y_R \theta_R} & \sigma^2_{\theta_R} \end{bmatrix} $$

The contours of equal probability of this pdf form ellipsoids in a 3 dimensional space, centered at the mean

location, $\hat{u}_R$. Although a complete analysis would have to consider the 3D ellipsoid, for localisation purposes, namely for the choice of visible landmarks and for the setting of the scanning parameters, two marginal pdf, for the vehicle's position and orientation, are considered.

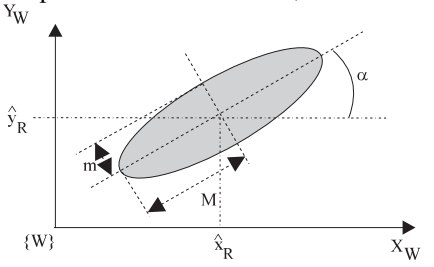

Fig.2.4 - 2-dimensional ellipse of error (robot position uncertainty)

The equal probability contour of robot's position in the world frame is a 2D ellipses as represented in Fig.2.4. Expressions for the length of half the major and minor axis, M and m, and the angle α that the major axis of the ellipses makes with the positive X-axis are given in [11].

3. Localisation algorithm

This section describes the main steps of the localisation algorithm whose structure is represented in Fig.3.1.

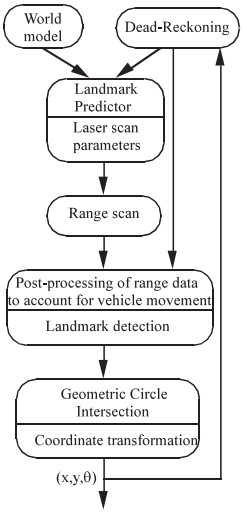

Fig.3.1 - Localisation algorithm

From a rough estimate of the mobile robot's position and orientation given by dead-reckoning and a quantification of the associated error, the algorithm,

- chooses two visible edges of the environment,
- defines the scanning parameters that will be used to perform a range profile acquisition,
- processes the acquired data, aiming at extracting the edges and estimating the distance and the orientation of the mobile robot relative to both edges,
- estimates the mobile robot's location by a geometric circle intersection followed by a coordinate transformation.

In the sequel these steps are described. Full details are presented in [8].

3.1. Landmark choice

Given a particular location estimate, ${}^{W}\hat{u}_R = (\hat{x}_R, \hat{y}_R, \hat{\theta}_R)$, and the associated error covariance matrix, two particular edges (or sub-edges) have to be chosen as the targets of the scanning procedure. The problem solution raises several questions:

i) from the vehicle location, and taking into account the error, the sub-set of vertical edges that is not on the shadow region of the PTU is evaluated by geometric reasoning.

ii) vertical edges on the visibility region of the scanning device may be occluded by objects or obstacles on the environment. The occlusion depends on the robot actual location and on the geometry of the testbed. Occluded edges and occluded parts of visible edges are excluded from the set of landmark candidates for the localisation procedure.

iii) from the set of visible edges (or sub-edges) containing all the potential candidates for the scanning procedure, two of them have to be chosen. The best choice, dictated by sensitivity considerations on the localisation procedure, is discussed in Section 4.

The position uncertainty is taking into account in the evaluation i) and ii) above by considering the edge's visibility from all the points in the shadowed region represented in Fig.2.4.

The outcome of the previous procedure is a pair of visible vertical edges, E_0 and E_1, with known coordinates in {W}. For both, it is known a rough estimate of the distance between the vertical lines containing the edge and the axis z_B of the PTU and the upper and lower z coordinates of the edge's visible part.

3.2. Scanning parameters

When the choice for the target edges is concluded, the parameters of the scanning device are to be defined taking into account the characteristics of the PTU and of the laser head. The key parameters for each scan are:

HScanCentroid, VScanCentroid
HScanWidth, VScanWidth
NpH, NpV

where HScanCentroid and VScanCentroid represent the pan and tilt angles corresponding to the centre of the solid angle that is going to be scanned, HScanWidth and VScanWidth are the pan and tilt ranges and NpH and

NpV represent the number of horizontal (for constant tilt) and vertical (for constant pan) scanning points.

A line scan, i.e., a scan done with a constant tilt angle, is sufficient for the detection of a vertical edge. Therefore, and for acquisition time minimisation, the two scans consider NpV=1, VScanWidth=0^{o}. The angle VScanCentroid is evaluated aiming at pointing the scanning device to any visible point of the edge.

The HScanWidth and the angle corresponding to the HScanCentroid are evaluated in such a way that the range for the pan angle contains the pan angles for which the edge under consideration is visible from all the points in the shadowed region in Fig.2.4, taking also into account the uncertainty on the orientation of the frame {B} relative to {W}. The number of range points in the line scan is given as,

$$NpH = \frac{HScanWidth \times (d / \cos(VScanCentroid))}{(\xi / \gamma)}$$

where d is a rough estimated distance between the vertical line containing the edge and the PTU vertical axis, ξ is the footprint dimension and γ is an over sampling factor. For γ>1, consecutive footprints will overlap.

3.3. Scanning direction

When the vehicle is stopped, the direction of the line scan (from left to right or from right to left) is irrelevant. However, when the vehicle is moving during a range acquisition, the scanning parameters have to be chosen in such a way that the target edge will be scanned even when each range sample is acquired at a different position of the base of the scanning device.

The two scans represented in Fig.3.2 have the same parameters except for the scanning direction. Both cases consider a straight line and uniform movement for the robot.

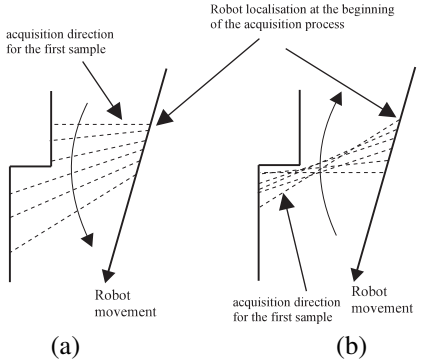

Fg.3.2- Range acquisition with a moving robot and different scanning directions

In case (a), where the scan direction follows the robot's movement the edge is detected. On the contrary, it is miss (case (b)). Therefore, the horizontal scan direction should be set to follow the robot's movement.

3.4. Edge scanning and detection

A range line profile contains NpH points, each of which corresponds to a particular pair of pan/tilt angles. For each pair, the laser head measures a range value r=r(θ_{pan}, θ_{tilt}). The x,y, z coordinates of the target that produced the acquired range, in the frame {B}, are obtained through a coordinate transformation that combines the rotations of θ_{pan} and θ_{tilt} of the frame {B}, and a translation to {B} of the frame associated with the LRF. From the set of detected points, expressed by their coordinates in the frame {B}, an edge detector is implemented, based on a geometric model fitting, [4], [10].

The outcome of the edge detector for the two scanned landmarks is

$$E_0 \rightarrow ({}^{B}\hat{x}_0, {}^{B}\hat{y}_0, \hat{\beta}_0) \text{ and } E_1 \rightarrow ({}^{B}\hat{x}_1, {}^{B}\hat{y}_1, \hat{\beta}_1)$$

where $({}^{B}\hat{x}_0, {}^{B}\hat{y}_0)$ and $({}^{B}\hat{x}_1, {}^{B}\hat{y}_1)$ are the coordinates of the detected edge points and $\hat{\beta}_0$ and $\hat{\beta}_1$ are the corresponding pan angles, all represented in {B}. From the range data associated with these points, the distance between the vertical line containing the edge point and the axis z_B is evaluated, leading to the two sets

$$E_0 \rightarrow (\hat{d}_0, \hat{\beta}_0), \qquad E_0 \rightarrow (\hat{d}_1, \hat{\beta}_1)$$

When the robot is moving during the range acquisition, each acquired measurement corresponds to a different location of the scanning device. Hence, a reference location is chosen, the acquired range data is corrected accordingly, and the edges extracted using the previous procedure. The robot motion is known, up to a certain confidence, provided that odometric data is available. The accumulated errors of the robot's location given by odometry will not influence the referred range correction, since only the differential movement relative to the reference location (fixed at the time instant of the acquisition of the first measurement) is used and given that, in the total acquisition time, the absolute displacement of the mobile robot is small.

3.5. Circle intersection and coordinate transformation

The localisation approach obtains the PTU location estimate as the intersection of two circumferences. A fixed coordination transformation, with parameters dependent on the vehicle's geometry, will then yield the robot's location.

For each of the chosen vertical edges, E_0 and E_1, the edge detector provided an estimated distance, $\hat{d}_0$ and $\hat{d}_1$, to the vertical axis of the frame {B}. Hence, the estimated position of the origin of this frame expressed in {W}, $(\hat{x}_{0B}, \hat{y}_{0B})$ is a solution, of the system of equations,

$$\left(\hat{x}_{o_B} - x_0\right)^2 + \left(\hat{y}_{o_B} - y_0\right)^2 = \hat{d}_0^2$$

$$\left(\hat{x}_{o_B} - x_1\right)^2 + \left(\hat{y}_{o_B} - y_1\right)^2 = \hat{d}_1^2$$

that represent the two circumferences in Fig.3.3. The coordinates of the centres of the circumferences, (x_0, y_0) and (x_1, y_1) defined in the world frame, are those of the projections of the chosen vertical edges in the XY plane of {W}, and consequently a priori known, and their radii, $\hat{d}_0$ and $\hat{d}_1$, are estimated as the result of the scanning procedure.

For $x_0 \neq x_1$, the solution of the above system yields,

$$\hat{x}_{o_B} = m\hat{y}_{o_B} + n,$$

where,

$$m = \frac{y_1 - y_0}{x_1 - x_0}$$

$$n = \frac{\hat{d}_1^2 - \hat{d}_0^2 + \left(x_0^2 - x_1^2\right) + \left(y_0^2 - y_1^2\right)}{2\left(x_0 - x_1\right)}$$

From the above relations,

$$\hat{y}_{o_B} = \frac{\left[m\left(x_0 - n\right) + y_0\right] \pm b}{1 + m^2}$$

$$b = \sqrt{(1+m^2)\hat{d}_0^2 - \{(n - x_0) + my_0\}^2}$$

When $x_0 = x_1$, the intersection is given by,

$$\hat{y}_{o_B} = \frac{\left(\hat{d}_0^2 - \hat{d}_1^2\right) + \left(y_1^2 - y_0^2\right)}{2\left(y_1 - y_0\right)}$$

$$\hat{x}_{o_B} = x_0 \pm \sqrt{\hat{d}_0^2 - \left(\hat{y}_{o_B} - y_0\right)^2}$$

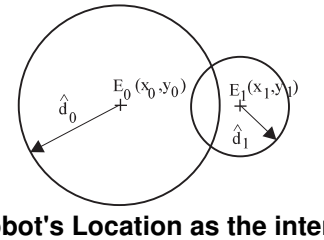

Fig.3.3 - Robot's Location as the intersection of two circumferences

The unique solution is chosen through the knowledge of the rough position estimate given by odometry. The orientation of the frame {B} relative to {W}, $\hat{\theta}_{o_B}$, is obtained either from $\hat{\beta}_0$ or $\hat{\beta}_1$. Its evaluation, corresponding to a trigonometric manipulation, is straightforward from Fig. 3.4.

A coordinate transformation from {B} to {R}

$$^W\hat{o}_B = (\hat{x}_{o_B}, \hat{y}_{o_B}, \hat{\theta}_{o_B}) \rightarrow {}^W\hat{u}_R = (\hat{x}_R, \hat{y}_R, \hat{\theta}_R)$$

yields the final estimate of the robot´s location in {W}.

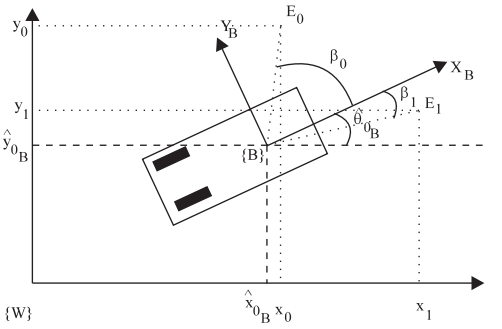

Fig3.4 - Evaluation of PTU orientation

4. Optimal choice of visible edges

From the set of visible edges, this section discusses the choice of two visible edges according to an optimisation criterion. The criterion accounts for the sensitivity of the location estimate relative to the edge estimation error.

Based on range data, the algorithm detects the vertical edges (whose presence was predicted beforehand) and estimates the distance of the robot to the corresponding edge, i.e., obtains estimated values, $\hat{d}_0$ and $\hat{d}_1$ of d_0 and d_1. The errors on $\hat{d}_0$ and $\hat{d}_1$ result from the precision of the LRF at that precise range and from the errors on the edge detector. Those errors will propagate into the robot's location estimate. Assuming that, with a given probability,

$$d_0 - \varepsilon < \hat{d}_0 < d_0 + \varepsilon,\ d_1 - \delta < \hat{d}_1 < d_1 + \delta$$

Fig. 4.1 - (a) shows how the distance error influence the location error. In Fig. 4.1-(a), the robot's location lies in one of the regions that result from the intersection of the two shadow circular bands.

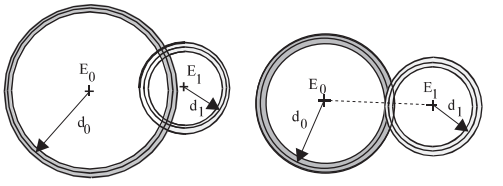

Fig.4.1 - Influence on the distance error on the estimate error. (a) general situation, (b) the robot lying in the line joining the two edges

The choice of the vertical edges aims at minimising the area of the intersection of the two circular bands. This area depends on the absolute values of d_0 and d_1, on the errors on their estimates, on the distance between the two edges, and on the robot's location relative to both edges.

For example, Fig. 4.1-(b) displays a situation that should be avoided in terms of landmarks' choice, where the robot is within the line joining both landmarks. From the simple example presented above it is clear that, for a given distance error, the robot's location error is minimised

when the two circular bands represented in Fig.4.1 intersect perpendicularly.

The perpendicular intersection of the circular bands results from a particular choice, where the line segments defined by the robot's position and the base of each edge are perpendicular. This choice yields when the robot lies in a circumference whose diameter is defined by the two edges, as represented in Fig. 4.2.

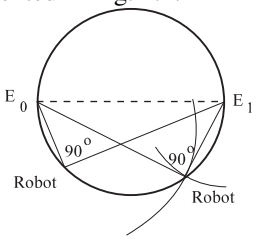

Fig.4.2 - Minimum error propagation situation

The previous criterion defines an optimal choice of the landmarks for localisation. It is clearly useful to discuss the degradation that occurs when this choice is not possible or not available. The degradation will again be stated in terms of the area of the intersection of the two circular bands as represented in Fig.4.1-(a). Taking into account the LRF allowable ranges and the associated errors, a reasonable approximation bounds the intersection area by a polygon. The polygon is a rectangle when the robot lies in the circumference whose diameter is defined by the two scanned edges and a parallelogram when the robot lies outside or inside the circumference, (see Fig.4.3).

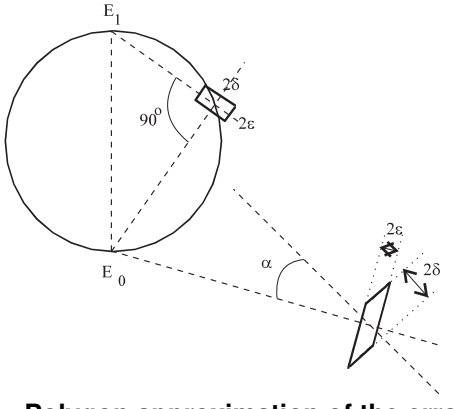

Fig.4.3 - Polygon approximation of the error area

The areas of the rectangle and parallelogram represented in Fig.4.3 are given by $4\delta\varepsilon/|\sin\alpha|$ which shows that the area grows with the inverse of $|\sin\alpha|$. When the robot is inside the circumference represented in Fig.4.3, the angle α is greater than 90^o, but the same result yields. It should be pointed out that the approximation by the polygon of the areas defined by the circular bands is no longer valid for $\alpha \cong 0^o$ and $\alpha \cong 180^o$. The choice of the minimum value of α clearly depends on the required precision for the localisation procedure.

A different issue relates with the performance of the edge detector to extract different types of edges. Fig. 4.4 displays two situations with the same map but different capture points. In (a), both edges E_0 and E_1 are visible. In (b), the single visible edge, E_1, suffers from the *mixed point* problem (see [10]) because the laser footprint crosses the edge between two objects. In this case the distance measurement is a combination of the distance to the two objects, leading to a more difficult edge detection.

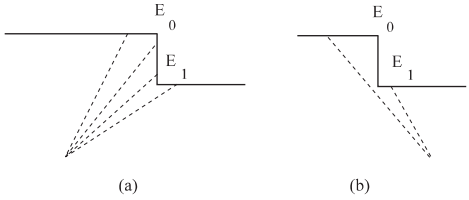

Fig.4.4 - Different types of edges according to the location of the capture point.

For the set of visible edges, the type of edge is a function of the robot's location. In the choice of the landmarks for localisation, situations as the one represented in Figure 4.4-(b) should be avoided.

5. Experimental results

This section presents a set of relevant results of the robot's location estimate for a still robot. In the assessment of a localisation algorithm, the estimated locations ought to be compared with the real ones, if they are available, either by means of a more precise localisation device/scheme or by direct measurement. This last option was adopted in the present work. Three different experiments were conducted.

Experiment 1. In this experiment, the robot had a fixed location around (*),

$$x_R = 1.97\text{m},\ y_R = 3.95\text{m},\ \theta_R = -45^o$$

as represented in Fig. 5.1, and seven different initial estimates were provided to the localisation algorithm, together with an associated standard deviation in position and orientation. For all the trials, the same pair of vertical edges (see Fig.5.1) were chosen as landmarks. The distance to the edges is 4.17m and 6.07m and the angle between the lines defined by the PTU vertical axis and each edge is 14.6^o.

The pairs of initial/estimated location are displayed in Table 5.1. Eventhough the number of independent experiments is very small to allow a statistical interpretation of the results, the sample mean and the sample standard deviation evaluated from the above estimates lead to

(*) errors on human measurement are considered.

Sample Mean ----> $\hat{x}_R$ = 1.977 m, $\hat{y}_R$ = 3.957 m, $\hat{\theta}_R$ = -47.36°
SampleStd.Dev.---> $\hat{\sigma}_{x_R}$ =0.020m, $\hat{\sigma}_{y_R}$ =0.021m, $\hat{\sigma}_{\theta_R}$ = 0.76°

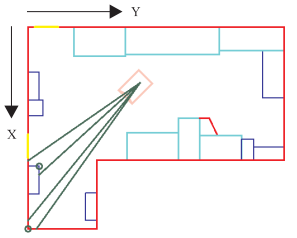

Fig.5.1 - Conditions for experiments 1 and 2

						Real Locat.		
						x(m)	y(m)	θ(deg)
						1.97	3.95	-45.00
Initial Locat. Estimate			Std.Dev. in Initial Location			Final Locat. Estimate		
x(m)	y(m)	θ(deg)	in x(m)	in y(m)	in θ(deg)	x(m)	y(m)	θ(deg)
2.00	4.00	-45.00	0.05	0.05	5.00	1.97	3.95	-47.10
2.10	4.05	-45.00	0.05	0.05	5.00	1.96	3.94	-47.37
1.85	3.85	-45.00	0.05	0.05	5.00	2.00	3.99	-47.69
2.00	3.85	-42.00	0.05	0.05	5.00	2.01	3.98	-47.72
1.90	4.00	-47.00	0.05	0.05	5.00	1.96	3.94	-47.48
1.95	3.95	-50.00	0.05	0.05	7.50	1.99	3.97	-45.75
1.90	4.00	-50.00	0.05	0.05	7.50	1.95	3.93	-48.41

Table 5.1 - Results of experiment 1

Experiment 2. In this experiment twenty five independent trials were performed aiming at obtaining a statistical characterisation of the localisation algorithm. For all the trials, the initial location and the associated standard deviation were assumed to be,

$$\hat{x}_R = 2.30 \text{ m}, \quad \hat{y}_R = 3.70 \text{ m}, \quad \hat{\theta}_R = -45^\circ$$
$$\sigma_{x_R} = 0.050 \text{ m}, \quad \sigma_{y_R} = 0.05 \text{ m}, \quad \sigma_{\theta_R} = 5^\circ$$

and the pair of scanned edges the ones represented in Fig. 5.1. The choice of the line scanning parameters, constant for the set of trials, lead to NpH=24, γ=1.0, HScanWidth=14.7°.

The sample mean and the associated standard deviation of the estimated locations are given by,

Sample Mean ----> $\hat{x}_R$ = 2.29 m, $\hat{y}_R$ = 3.73 m, $\hat{\theta}_R$ = -47.24°
Sample Std.Dev.---> $\hat{\sigma}_{x_R}$ =0.023m, $\hat{\sigma}_{y_R}$ =0.024m, $\hat{\sigma}_{\theta_R}$ = 0.54°

showing a decrease on the location uncertainty as the result of the proposed algorithm, namely in what concerns the robot orientation.

Experiment 3. The third experiment refers to the influence of the pair of chosen vertical edges that will act as the natural landmarks. This subject is related with the optimisation choice of the scanned edges, discussed in Section 4. The three situations displayed in Fig. 5.2 were considered for a robot real location (evaluated manually from the position of both wheels)

$$x_R = 1.81\text{m}, \quad y_R = 3.82\text{m}, \quad \theta_R = -1.7^\circ$$

and for which the initial location estimate provided as a rough estimate to the algorithm was

$$\hat{x}_R = 1.80 \text{ m}, \quad \hat{y}_R = 3.80 \text{ m}, \quad \hat{\theta}_R = 0^\circ$$

with $\sigma_{x_R} = 0.05$ m, $\sigma_{y_R} = 0.05$ m, $\sigma_{\theta_R} = 5^\circ$.

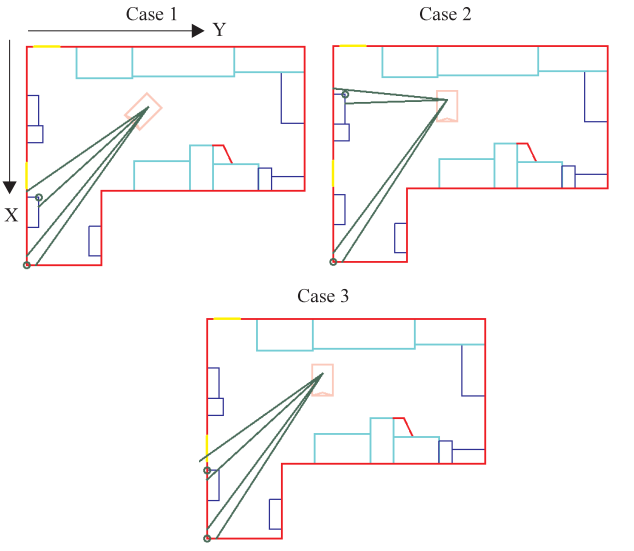

Fig.5.2 - Conditions for experiment 3

Taking as a reference the mobile robot real location, Table 5.2 displays, for each case, the distance of the PTU to the edges and the angles between the lines defined by the vertical axis of the PTU and each edge.

	Distance to Edges (m)		Angle Between
	E_0	E_1	Edges (deg)
Case 1	4.37	6.25	14.3
Case 2	3.53	6.25	63.0
Case 3	4.7	6.25	17.2

	Scanning Parameters					
	E_0			E_1		
	HScanWidth (deg)	HScanCentroid (deg)	NpH	HScanWidth (deg)	HScanCentroid (deg)	NpH
Case 1	14.0	-52.4	26	12.8	-38.2	34
Case 2	12.8	-101.1	19	12.8	-38.2	34
Case 3	13.7	-55.4	28	12.8	-38.2	34

Table 5.2 - Geometric and scanning parameters - experiment 3

The estimated locations are displayed in Table 5.3, showing that the best result was obtained in case 2 when the chosen landmarks are the most far apart.

			Real Location		
			x(m)	y(m)	θ(deg)
			1.81	3.82	-1.7
Initial Location		Estimate	Final Location		Estimate
x(m)	y(m)	θ(deg)	x(m)	y(m)	θ(deg)
1.80	3.82	0.0	1.83	3.86	-3.87
1.80	3.82	0.0	1.78	3.81	-3.16
1.80	3.82	0.0	1.75	3.77	-4.09

Table 5.3 - Results of experiment 3

6. Conclusions and future work

The proposed localisation procedure relies on the set of vertical edges of the environment. Being supported on natural landmarks, this means that no special adaptation of the environment has to be done before the robot's operation. This is important in many circumstances, namely when operation is to be done in dangerous or inaccessible environments to humans where it is not possible/easy to install and maintain artificial landmarks.

One of the critical issues of the proposed procedure is the choice of a good pair of edges for localisation. The paper derives the conditions for an optimal choice and discusses the degradation when the optimum cannot be achieved. The criterion minimises/evaluates the robot's position error for a given error on the detection of the landmark. The orientation estimate is a function of the position estimate and of the angle for which one of the chosen edges was detected and therefore reflects the angular resolution on the edge scanning and detection.

The spatial resolution on range data acquisition is another issue that has to be taken into account. For a given time-of-flight LRF device, this resolution may be increased by controlling the pan velocity of the PTU and allowing for overlapping footprints. However, smaller footprints yields better range accuracy for the coverage of the same pan angle leading to smaller errors on edge detection and location.

The experimental results, for a stopped robot, display a good performance both in position and orientation. For landmarks with a location far from the optimum, a robot location estimate was obtained within errors of ±2.5cm in x and y and $\pm 1^{o}$ (maximum) in θ. From the sensitivity analysis made in Section 4, an increased performance in x and y will be obtained for a better choice of the pair of landmarks, even though with no significative improvement on the orientation estimate. This will result from the use of a LRF with a smaller footprint.

When localisation is performed during robot's movement, the time interval necessary for the choice, scanning and detection of each edge has to be small. In other words, the robot's displacement during this interval has to be small to ensure that the scanning parameters established for a given robot's location will still allow the detection of the chosen edge based on rage data acquired at different robot's locations. The trade-off is clearly established in terms of the time of acquisition plus processing and the robot's speed. For the available experimental set-up the bottleneck corresponds to the data acquisition process, given that a measuring time of 50ms was settled for each single measurement. The option for a smaller integration time will decrease the accuracy of the range measurements, which will introduce larger errors on edge detection and consequently on the evaluation of the distance to the edge. The actual state-of-the-art LRFs provide shorter integration time for the same range accuracy, allowing higher robot's speed.

Future work will statistically quantify the edge detection performance for different view points, providing quantitative data for the statistical assessment of the localisation procedure. This information can be used to set, in real-time, the most appropriate acquisition conditions, in particular the choice of the scanning edges and angles and the adjustment of the robot's speed. An alternative non-optimal approach for landmark choice during robot movement will be investigated.

References

[1] J. Crowley, "World Modeling and Position Estimation for a Mobile Robot Using Ultrasonic Ranging, " 1989 IEEE Int. Conf. on R&A, Arizona, USA, May 1989, pp.674-680.

[2] I.J.Cox, "Blanche: Position Estimation for an Autonomous Robot Vehicle," Proc. of the IEEE/RSJ Int. Workshop on Robots and Systems (IROS'89), Sept. 1989, Tsukuba, Japan, pp.432-439.

[3] L.Feng, J.Borenstein, H.R.Everett, "Sensors and Methods for Autonomous Mobile Robot Positioning," Technical Paper UM-MEAM-94-21, University of Michigan, Dec.1994.

[4] Y.G.Leclerc, S.W.Zucker, "The Local Structure of Image Discontinuities in One Dimension," IEEE Trans. on PAMI, Vol.9, No.3, pp.341-355, 1987.

[5] J. J. Leonard, H. F. Durrant-Whyte, "Mobile Robot Localisation by Tracking Geometric Beacons," IEEE Trans. on Robotics and Automation, Vol.7, No.3, June 1991.

[6] Jae H.Kim, Hyung S. Chuo, "Experimental investigation for the estimation of a mobile robot's position by linear scanning of a landmark," Robotics and Autonomous Systems, 13(1994), 39-51.

[7] F. Pedrosa, M. I. Ribeiro, "Sonar Data Processing for the Navigation of a Mobile Robot," Proc. of the 5th Int. Conf. on Signal Processing Applications and Technology, Dallas, USA, Oct. 1994.

[8] M.I.Ribeiro, J.G.M.Gonçalves, “Mobile Robot Localisation using Laser Range data,” Techical Note No.I.96.44, ISIS, JRC, Feb. 96.

[9] V.A.Sequeira, J. G. M. Gonçalves, "Position estimation of a Mobile Robot Using Laser Range Data," Technical Note No.I.93.132, ISEI, JRC, October 1993.

[10]V.Sequeira, J. G. M. Gonçalves, M. I. Ribeiro, "3D Environment Modeling using Laser Range Sensing," Proc. of the Int. Symposium on Intelligent Robotic Systems, IRS'94, Grenoble, July 1994, pp.238-245.

[11]Randall C. Smith, Peter Cheeseman, "On the Representation and Estimation of Spatial Uncertainty," International Journal of Robotics Research, Vol.5, No.4, pp.56-68, 1986.

Acknowledgments

The first author acknowledges the Commission of the European Communities - Joint Research Centre for the grant that supported her work, done in the framework of the SMART network of the Human Capital and Mobility Programme.